applied sciences

MDPI

Article

Formulation and Evaluation of Hydrogels Based on Sodium Alginate and Cellulose Derivatives with Quercetin for Topical Application

Beata Szulc-Musioł [1,*], Wioletta Siemiradzka [2] and Barbara Dolińska [2]

[1] Department of Pharmaceutical Technology, Faculty of Pharmaceutical Sciences in Sosnowiec, Medical University of Silesia in Katowice, Kasztanowa 3, 41-200 Sosnowiec, Poland
[2] Department of Pharmaceutical Technology, Faculty of Pharmaceutical Sciences in Sosnowiec, Medical University of Silesia in Katowice, Poniatowskiego 15, 40-055 Katowice, Poland
* Correspondence: bszulc@sum.edu.pl; Tel.: +48-(32)-2699820

Abstract: Topical drug delivery in skin diseases provides a non-invasive, direct application of treatments to the affected area and avoids systemic toxicity. Quercetin is a natural polyphenol with documented activity to alleviate the symptoms of many skin diseases. The objective of this study was to prepare and assess the physicochemical properties of hydrogels made of sodium alginate (SA) and cellulose derivatives (methyl cellulose (MC) and carboxymethyl cellulose (CMC)), containing different concentrations of quercetin (0.4 and 0.7%). The physicochemical evaluation of the obtained hydrogels included organoleptic evaluation, texture analysis, spreadability, rheological properties, pH, and stability. Among the prepared formulations, MC-based gels had the highest viscosity, adhesiveness, cohesiveness, and stickiness. The results of this study indicate that MC-based hydrogels were superior to CMC- or SA-based gels in their ability to effectively deliver quercetin to the porcine skin ex vivo. The amount of quercetin retained in the skin after application of MC-based preparations containing higher concentrations of quercetin was 2.04-fold higher for CMC-based hydrogels and 2.6-fold higher for SA-based hydrogels.

Keywords: hydrogels; rheological properties; quercetin; sodium carboxymethyl cellulose; sodium alginate; methylcellulose; skin retention; texture analysis; stability of hydrogels; topical application

check for updates

Citation: Szulc-Musioł, B.; Siemiradzka, W.; Dolińska, B. Formulation and Evaluation of Hydrogels Based on Sodium Alginate and Cellulose Derivatives with Quercetin for Topical Application. *Appl. Sci.* **2023**, *13*, 7826. https://doi.org/10.3390/app13137826

Academic Editors: Artur Turek and Eva Martins

Received: 30 May 2023
Revised: 27 June 2023
Accepted: 28 June 2023
Published: 3 July 2023

Copyright: © 2023 by the authors. Licensee MDPI, Basel, Switzerland. This article is an open access article distributed under the terms and conditions of the Creative Commons Attribution (CC BY) license (https://creativecommons.org/licenses/by/4.0/).

1. Introduction

Quercetin is a plant-derived compound belonging to the flavonols group, which are flavone derivatives containing a hydroxyl group in the molecule connected to a carbon atom in the third position. Quercetin is one of the most widespread flavonoids in the plant world [1].

Due to its pharmacological and biological activities, quercetin has a significant role in the prevention of cardiovascular diseases, obesity, type 2 diabetes, asthma, cancer, viral infections, mood disorders, and many others [2–10]. Its anti-inflammatory and anti-ulcer effects have been demonstrated [11–14]. It stimulates neurogenesis and has been shown to improve memory [12,15,16]. The intake of a quercetin-rich diet reduces the risk of myocardial infarction and avoids varicose veins and atherosclerotic lesions by sealing blood vessel walls [17–20]. In the case of quercetin, it has been proven to reduce venous spider veins through its effect on cyclooxygenase activity, while its inhibition of the hyaluronidase enzyme contributes to a reduction in oedema [21]. This natural polyhydroxy flavonoid is classified as an effective antioxidant, diminishing the secretion of pro-inflammatory cytokines (IL-1 β, IL-6, TNF-α), chemokines, and nitric oxide [22].

Skin diseases are usually treated using topical formulations: ointments, creams, hydrogels.

A key problem with topical drug delivery is that only a small number of APIs can overcome the biological barriers in the human body. The skin acts as an external natural

barrier to protect against dangerous external agents such as microorganisms and chemicals. Crucial in this protection is the stratum corneum, which is in direct contact with the environment. Thanks to its special and well-ordered structure, it acts as an efficient barrier and determines the rate of the transdermal diffusion of drug molecules.

Quercetin, like other flavonoids, has been shown to have a number of beneficial effects on human skin, which may, among others, inhibit oxidative stress and inflammatory processes, prevent cancer, and reduce skin aging [23,24].

Several tests have demonstrated the anti-allergic effects of this natural polyphenol by inhibiting histamine release from basophils and mast cells, as well as via the inhibition of pro-inflammatory cytokines and interleukin-4 (IL-4) and IL-13,15 [25,26].

Pretreatment with quercetin in an experimental atopic dermatitis model resulted in faster wound healing through the mitogen-activated protein kinase (MAPK)/extracellular signal-regulated kinase (ERK) and NF-κB pathways. The authors of the study observed that this natural compound improved wound healing and regeneration of skin damaged by atopic dermatitis more effectively than dexamethasone [27].

As a result of its protective action on the skin, quercetin is an ingredient in skin care products in the form of a plant extract or in combination with other bioactive compounds. Quercetin has been proven to slow down UV-induced skin aging, dyspigmentation, and carcinogenesis [28–31]. Quercetin may also act as a chemopreventive agent by initiating cancer cell growth arrest, reducing tumor incidence and normal cell differentiation [32–35]. The study by Shin et al. also showed that quercetin inhibited the MAPK, Akt, and STAT3 signaling pathways. Furthermore, the authors revealed that quercetin directly targets the protein kinases JAK2 and PKCδ, preventing photo-aging in human skin [36].

In an in vivo study, Bagde et al. showed that the topical application of a quercetin nanogel with TiO_2 before exposure to UV radiation resulted in a significant reduction in the mean number of tumor nodules (3.63-fold) and mean tumor volume compared to the control group. However, in the Western blot analysis, a decrease in the expression of COX-2, EP3, EP4, cyclin D1, and PCNA was observed in the study group [28]. Another study found that the use of quercetin fatty acid esters increased cell–cell adhesion forces and had a higher apoptosis effect compared to the unconjugated form [37].

Many reports indicate an important supportive function for quercetin in the mechanism of wound healing [38,39]. This natural flavonoid has a broad spectrum of antibacterial properties but also has significant inhibitory effects on fungi, viruses, and parasites [40–43]. Quercetin destroys the bacterial cell wall or changes its permeability. In addition, it can prevent bacterial adhesion and weaken biofilm formation [40,44].

Water-soluble polymers of semisynthetic—methyl cellulose (MC), carboxymethyl cellulose (CMC)—and natural origin—sodium alginate (SA)—are used as gelling agents to prepare dermatological hydrogel-type formulations. SA is an anionic polysaccharide in which the carboxyl groups present in its structure interact with divalent metal cations such as Ca^{2+} to form a stable gel network [45]. It is a biomaterial with numerous applications in the pharmacology, cosmetics and biomedical fields. This polymer is used in many studies to obtain composite scaffolds that may have future applications in tissue engineering [46,47]. Yao et al. developed a scaffold of polycaprolactone and SA loaded with melatonin for tendon repair [48]. The authors observed that slow-release melatonin inhibited ROS production and macrophage infiltration and activated the Nrf-2/HO-1 signaling pathway. A high antioxidant capacity, higher in comparison to the base matrix (on average by 30 %), was determined for hydrogels based on cellulose, collagen, and SA with quercetin, anthocyanins, and lipoic acid [49]. The growing interest in this natural flavonoid is associated with its antimicrobial activity and biodegradability, as well as its low production costs. In an animal model, it was shown that exosomes, incorporated into an alginate hydrogel, accelerated wound closure, collagen synthesis, and vascularization in the injury area [50]. A hydrogel consisting of SA and platelet-rich plasma also showed high wound closure efficacy [51]. In contrast, another study showed that SA-based hydrogel membranes containing gallic acid were effective in inhibiting biofilm formation [52]. The presence of silver nanoparticles

in a tragacanth–alginate hydrogel enhanced, in a concentration-dependent manner, its antibacterial effects against planktonic and biofilm-forming efficiency [53].

The cellulose ethers, MC and CMC, are also of great interest both scientifically and commercially. Thanks to attributes such as biodegradability, biocompatibility, and low production inputs, they are often used in the preparation of hydrogels, patches, and medical devices [54–58].

The aim of this work was to prepare hydrogels based on semisynthetic (MC, CMC) and natural polymers (SA) that deliver API to the skin with the potential to be used in the treatment of dermatological diseases. Hydrogels containing quercetin at two concentrations (0.4% and 0.7% wt/wt) were prepared, and the effects of the type of polymer and API content on their physicochemical properties, as well as the amount delivered through the skin or retained in the skin reservoir ex vivo, were assessed.

2. Materials and Methods

2.1. Materials

Quercetin (Cayman Chemical Company, MI, USA); MC (viscosity of 2% solution at 25 °C: 3755 mPa.s; Sigma Aldrich, Inc. St. Louis, MO, USA); SA (viscosity of 2% solution at 25 °C: ~250 cps; Biomus, Lublin, Poland); CMC (viscosity of 2% solution at 25 °C: 400–800 cps; Sigma Aldrich, Inc. St. Louis, MO, USA); glycerol 85% (Galfarm, Kraków, Poland); calcium chloride (Avantor Performance Materials Poland S.A., Gliwice, Poland); dimethyl sulfoxide (Gaylord Chemical Company, L.L.C., USA); potassium dihydrogen phosphate (Avantor Performance Materials Poland S.A., Gliwice, Poland); disodium hydrogen phosphate anhydrous (Avantor Performance Materials Poland S.A., Gliwice, Poland); sodium chloride (Avantor Performance Materials Poland S.A., Gliwice, Poland); water for injection (Galfarm, Krakow, Poland); ethyl alcohol 96% (Avantor Performance Materials Poland S.A., Gliwice, Poland); and phosphate-buffered saline (PBS) (Biomed, Lublin, Polska). All materials used in the study were of the analytical grade and satisfy the requirements of standards and certificates.

2.2. Methods

2.2.1. Formulation of the Hydrogel

Formulations based on MC and CMC were made by hot dispersion of the gellating agent in a mixture of water and glycerol heated to 80 °C for the MC-based formulation and to 50 °C for the CMC-based formulation.

Then, under ambient conditions, polymers were incrementally added to the solution and stirred until the mixtures were homogeneous (300 rpm). The procedure for obtaining formulations based on SA was to dissolve it in a mixture of water and glycerol with 200 µL 0.5% solution of calcium chloride (crosslinking agent) at ambient temperature. Quercetin, after dissolving in dimethyl sulfoxide (DMSO), was introduced into the prepared formations. The active ingredient solution was mixed with a hydrogel base via mechanical stirring for 15 min. The obtained hydrogels were placed in the polyethylene containers and left in a refrigerator for further examination. The compositions of the hydrogels are presented in Table 1.

2.2.2. Visual and Sensory Inspection of Prepared Formulations

The prepared hydrogel formulations were inspected visually for their color, appearance, uniformity and consistency, stickiness, greasiness and greasing, and adhesion [59]. The method of performing the tests was previously described by Siemiradzka et al. [60].

2.2.3. pH Determination

The pH of the quercetin gels was determined in triplicate using a Seven Compact S210 calibrated pH meter, (Mettler Toledo, Switzerland) equipped with an InLab Routine Pro-ISM electrode. Data are presented as mean ± SEM.

Table 1. The composition of hydrogels with quercetin.

Ingredient (g)	Formulation Designation					
	F-AA	F-CA	F-MA	F-AB	F-CB	F-MB
	Content (g)					
Quercetin	0.4	0.4	0.4	0.7	0.7	0.7
Sodium alginate	4.0			4.0		
Methylcellulose	-	-	4.0	-	-	4.0
Sodium carboxymethyl cellulose	-	4.0	-	-	4.0	-
Glycol 86%	10	10	10	10	10	10
Dimethyl sulfoxide	2	2	2	2	2	2
Purified water	up to 100	up to 100	up to 100	up to 100	up to 100	up to 100

F-AA, F-AB—hydrogels based on SA; F-CA, F-CB—hydrogels based on CMC; F-MA, F-MB hydrogels based on MC.

2.2.4. Spreadability Test

Using a sterile syringe, 1 mL of the prepared hydrogel was applied to the glass plate. The formulation was covered with a calibrated plate, on the surface of which weights of increasing mass were placed: 20, 50, 100, 200, 300, 400, 500, 600 g. The radii of the gels were measured 20 s after placing the next weight. The results obtained allowed the area occupied by the prepared hydrogels to be calculated according to the following formula:

$$P = \pi r^2$$

where P—surface area occupied by the hydrogel (m^2); r—radius of the hydrogel (cm).

Spreadability tests of developed hydrogel were carried out in triplicates at room temperature.

2.2.5. Rheology Measurements

The rheological parameters of the prepared hydrogel formulations were assayed using a RM 200 Touch rotational rheometer (Lamy Rheology Instruments, Champagne au Mont d'Or, France) with an MK-CP 2445 measuring system, a parallel plate geometry (diameter 35 mm, gap 1.0 mm) and a CP-1 Plus laboratory thermostat. The flow and the viscosity curves were performed in a controlled shear mode in the range 5.0–100.0 s^{-1} within a time of 100 s. Rheology measurements of hydrogel formulations were carried out in six repetitions at 32 ± 0.5 °C. Using the hysteresis loop test, flow and viscosity curves were plotted.

2.2.6. Texture Analysis

The texture profile analysis (TPA) and compression properties of hydrogel samples were measured using a texture analyzer (TX-700, Lamy Rheology Instruments, Champagne au Mont d'Or, France) equipped with ½ spherical probe with a diameter of 8 mm. The probe was squeezed at a speed of 1 mm/s for a range of 5 mm into the hydrogel and removed. The pretest and post-test speeds were both 0.1mmm/s, and the force for the probe to start was 0.05 N. The time interval of 20 was set between the two compression cycles. The hardness matches the highest force in the first stage of compression, and cohesiveness, adhesion, and elasticity are defined in Figure 1. Adhesiveness determines the work required to overcome the forces of attraction between the material being tested and the probe surface. Cohesiveness expresses the ratio of work performed to compress the sample during the first and second A2/A1 cycles. Elasticity determines the D2/D1 ratio between two compression phase distances. Data acquisition and analysis were carried out using the Rheotex software, version TX-UK01/2019. The measurement temperature was

25 °C. For each of formulation, the test was measured six times. Ts and YM were derived by applying the formulas below:

$$T_S = \frac{F\ (\mathrm{N})}{A\ (\mathrm{m}^2)} \quad (1)$$

$$YM = \frac{T_S}{\frac{\Delta l}{l}} \quad (2)$$

where F (N) is the force imposed on the gel, A (m^2) reflects the computed cross-sectional area of the gel, Δl (m) is the length strain, and l (m) reflects the initial length of the sample.

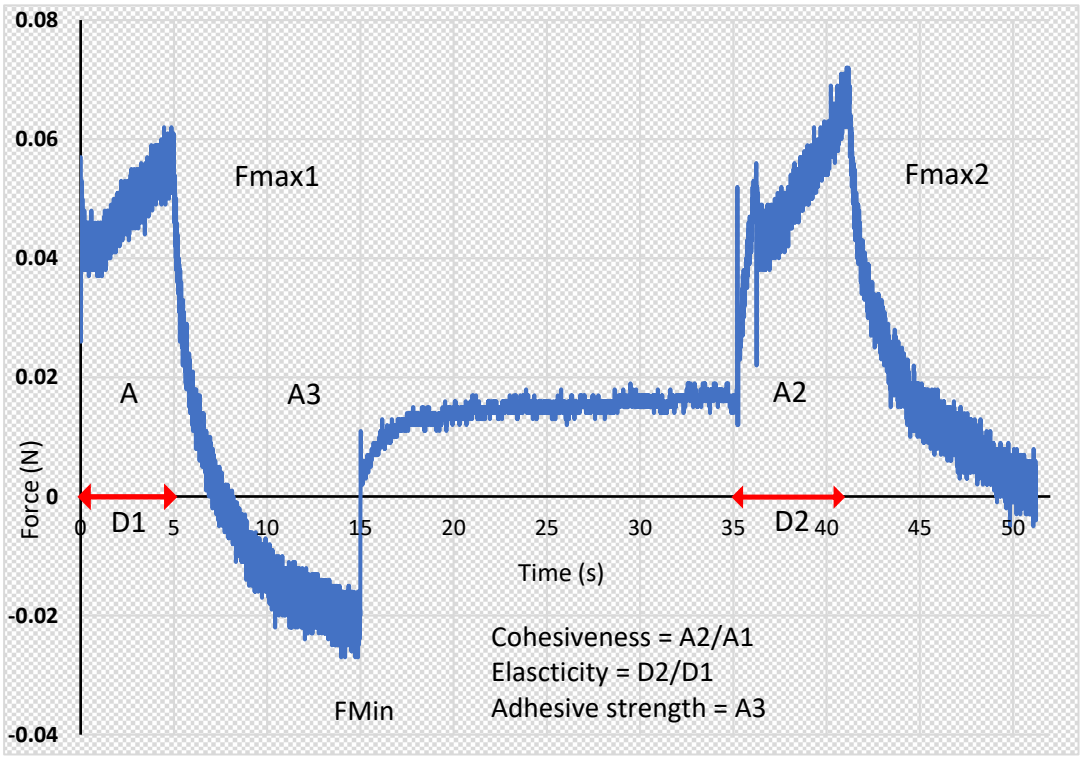

Figure 1. Representative picture of data of texture analysis of quercetin hydrogels.

2.2.7. Stability Test

The six formulations with quercetin were kept in polyethylene boxes at a temperature of 2 °C to 8 °C for 28 days. After this time, the hydrogel samples were visually assessed for formulation appearance and evaluated for chemical stability (pH, API content) and physical stability (color, pH, spreadability, texture, viscosity).

2.2.8. Ex Vivo Skin Permeation Experiments

Skin permeation experiments were performed with a handheld Franz Cell diffusion apparatus (Perme Gear, Hellertown, PA, USA) using vertical diffusion Franz cells with an effective permeation diameter of 0.636 cm. Porcine skin samples were obtained from a local abattoir. Subcutaneous fat and hair were removed from the skin. Skin fragments measuring 1.1 cm × 1.1 cm were washed with a 0.9% NaCl solution until an absorbance of A < 0.02 was obtained and then mounted in diffusion cells (temperature 37.0 ± 0.2 °C). Next, a 0.2g hydrogel sample was placed on the skin, facing the stratum corneum into the donor compartment. A mixture of ethanol (96% *v/v*) and PBS in a ratio of 40:60 *v/v* was used as acceptor fluid in a volume of 5 mL [61]. At predetermined times (after 1, 2, 4, 8, 12, and 24 h), acceptor solution in a volume of 2 mL was taken through the sampling port of the Franz diffusion cell, and the same volume of fresh acceptor solution was added. The samples were analyzed for absorbance at a wavelength of 373 nm using the Cecil CE

3021 UV-VIS spectrophotometer (Cecil Instruments Limited, Cambridge, UK), and the concentration of quercetin was calculated from the standard curve. Each formulation was tested six times.

To determine the amount of API remaining in the skin, residual hydrogels were removed from the skin, washed a few times with 3 mL PBS, and then wiped 4 times with paper soaked in ethanol and dried with filter paper. After washing, the skin was cut into small pieces, flooded with 5 mL ethanol, and shaken for 4 h on the Compact Shaker KS15 (Edmund Bühler GmbH, Bodelshausen, Germany) to extract the API residue. A blank of untreated skin was prepared in the same way as treated skin. In control experiments carried out previously, in which the quercetin hydrogel preparations were removed immediately after application and the skin was extracted with ethanol, the validity of such a cleansing procedure was confirmed.

The concentrations of extracted quercetin were determined spectrophotometrically, and the data were expressed as the amount of quercetin per area ($\mu g/cm^2$).

2.2.9. Statistical Analysis

A statistics software (Statistica 13.0, STATSOFT; Statistica, Tulsa, OK, USA) was used to perform all statistical analyses. Experimental data were expressed as mean (M) with standard deviation (SD). One-way ANOVA followed by the use of Tukey's multiple comparison tests were employed to test the difference between groups; $p < 0.05$ was considered significant.

3. Results

3.1. Visual and Sensory Inspection of Prepared Formulations

All the obtained hydrogels were yellow. The different quercetin content of the hydrogel medium had little effect on the color intensity. However, the use of different types of gelling agents results in a different smell, consistency, stickiness, and force of adhesion. Images of freshly prepared hydrogels are given in Figure 2. Sensory evaluation parameters of formulated hydrogels, namely color, consistency, homogeneity, adhesion, stickiness, greasiness, greasing, and pillow effect, are presented in Table 2.

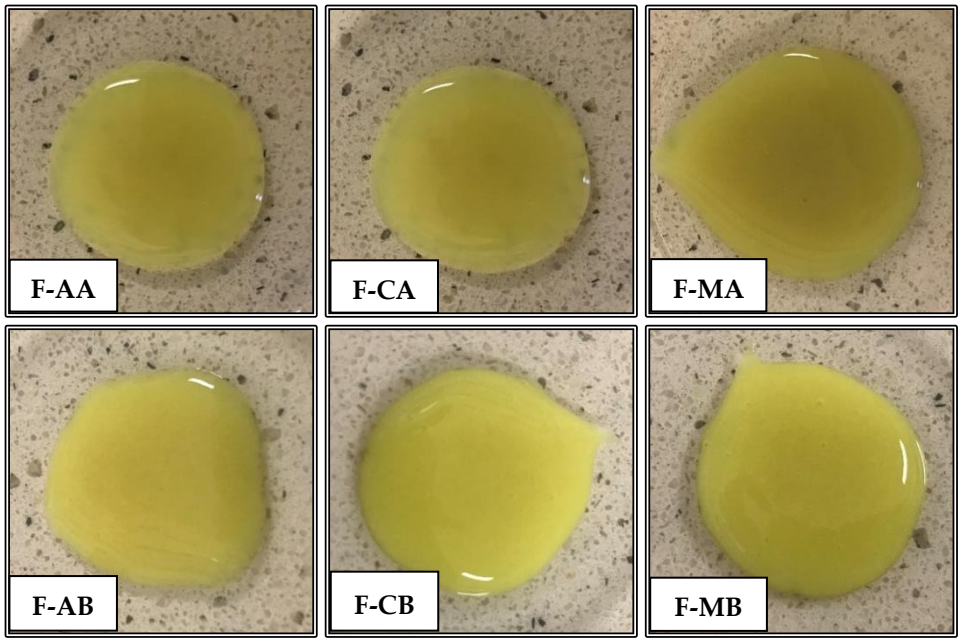

Figure 2. Photographs of prepared quercetin hydrogels (1:1). F-AA (SA; quercetin 0.4%), F-AB (SA; quercetin 0.7%), F-CA (CMC, quercetin 0.4%), F-CB (CMC, quercetin 0.7%); F-MA (MC, quercetin 0.4%); F-MB (MC, quercetin 0.7%).

Table 2. Results of the organoleptic tests of the quercetin formulations.

F-AA	F-CA	F-MA	F-AB	F-CB	F-MB
Color					
yellow	yellow	yellow	intensified yellow	intensified yellow	intensified yellow
Consistency					
very gentle semi-solid	very gentle semi-solid	very gentle semi-solid	very gentle semi-solid	soft semi-solid	soft semi-solid
Homogeneity					
homogenous	homogenous	homogenous	homogenous	homogenous	homogenous
Adhesion					
picks up easily, does not flow, forms a persistent typical cone on the fingertip	more difficult to pick up no characteristic cone	picks up easily, does not flow, forms a persistent typical cone on the fingertip	picks up easily, does not flow, forms a persistent typical cone on the fingertip	more difficult to pick up no characteristic cone	picks up easily, does not flow, forms a persistent typical cone on the fingertip
Stickiness (0–5)					
medium sticky sticky (3/5)	moderately sticky (1/5)	medium sticky (3/5)	Medium sticky (3/5)	not sticky (0/5)	medium sticky (3/5)
Greasiness and greasing					
no oily film when applied	no oily film when applied	no oily film when applied	no oily film when applied	no oily film when applied	no oily film when applied
Pillow effect					
slight layer of formula felt on fingers	slight layer of formula felt on fingers	slight layer of formula felt on fingers	slight layer of formula felt on fingers	slight layer of formula felt on fingers	slight layer of formula felt on fingers

F-AA (SA; quercetin 0.4%), F-AB (SA; quercetin 0.7%), F-CA (CMC, quercetin 0.4%), F-CB (CMC, quercetin 0.7%); F-MA (MC, quercetin 0.4%); F-MB (MC, quercetin 0.7%).

3.2. pH Determination

The acidic character of the skin plays an important role in skin barrier regeneration and antimicrobial response [62,63]. The pH of the skin is influenced by many factors of both exogenous origin (e.g., cosmetics, detergents, dermatological drugs) and endogenous origin (sweat composition, sebum secretion intensity, sex, age). However, maintaining an acidic pH is beneficial for the physiology of the epidermis and the skin microflora, and avoids damaging the lipid barrier and the integrity of the stratum corneum [64].

In the study, the lowest pH values determined for the MC-based formulations were 4.62 ± 0.02 and 4.51 ± 0.04 for F-MA and F-MB, respectively, while the highest values for CMC-based formulations were 6.40 ± 0.01 and 6.39 ± 0.01 for F-CA and F-CB, respectively (Table 3). The pH values determined for the formulations prepared ranged from 4.51 to 6.40, which corresponds to the physiological pH of the skin and indicates the formulations can be applied to the skin without causing irritation during application.

Table 3. Spreadability and pH of prepared quercetin hydrogels.

Formulation Code	Spreadability (mm^2)	pH
F-AA	304.70 ± 6.80^{c}	5.62 ± 0.02
F-CA	327.30 ± 12.06^{a}	6.40 ± 0.01
F-MA	273.76 ± 3.15^{d}	4.62 ± 0.02
F-AB	$269.96 \pm 0.22^{a,e}$	5.60 ± 0.02
F-CB	295.50 ± 5.93^{b}	6.39 ± 0.01
F-MB	$256.03 \pm 5.15^{a,f}$	4.51 ± 0.04

[a] $p \leq 0.05$ as compared to F-AA, F-MA; [b] $p \leq 0.05$ as compared to F-AB, F-MB; [c,d] $p \leq 0.05$ as compared to F-CA, [e,f] $p \leq 0.05$ as compared to F-CB. F-AA (SA; quercetin 0.4%), F-AB (SA; quercetin 0.7%), F-CA (CMC, quercetin 0.4%), F-CB (CMC, quercetin 0.7%), F-MA (MC, quercetin 0.4%), F-MB (MC, quercetin 0.7%).

3.3. Spreadability Test

The even distribution of the product on the skin is influenced by its spreadability. A measure of this parameter is the increase in surface area of the hydrogel under applied pressure. The ease of spreading the gel enables patient compliance and facilitates its even application on the skin. It was found that hydrogels based on CMC had the highest spreadability (327.30 ± 12.066 F-CA; 295.50 ± 5.93 F-CB) and the ones based on MC had the lowest (273.76 ± 3.15 F-MA; 256.03 ± 5.15 F-MB) (Table 3).

An increase in the API content in hydrogel formulations caused a significant decrease ($p \leq 0.05$) in their spreadability. With respect to spreadability, the prepared gel formulations could be grouped in ascending order, as follows: F-CA < F-AA < F-CB < F-MA < F-AB < F-MB.

3.4. Apparent Viscosity

Table 4 shows the results of viscosity measurements (η) of quercetin formulations, at the following shear rates: 30 s^{-1}, 60 s^{-1}, 100s^{-1}. The viscosity value determined for the tested formulations at all applied shear rates increased in the following sequence: F-CA < F-CB < F-AA < F-AB < F-MA < F-MB. It was observed that the MC-based formulations showed significantly higher viscosity than the other formulations. With regard to the viscosity at a shear rate of 30s^{-1}, for preparations with a lower API content, the viscosity of F-MA was higher by 47.65% ($p \leq 0.01$) and 13.16% ($p \leq 0.01$) vs. F-CA and F-AA, respectively, while for preparations with higher API content, the viscosity of F-MB was higher by 58.06% ($p \leq 0.01$) and 32.97% ($p \leq 0.01$) vs. F-CB and F-AB, respectively. In addition, it was shown that increasing the quercetin concentration in MC-based hydrogel formulations increased their viscosity significantly ($p \leq 0.05$). The viscosity curves obtained for the tested formulations are shown in Figure 3.

Table 4. Apparent viscosity of prepared hydrogels depending on the shear rate (η).

Formulation Code	η (30 s^{-1})	η (60 s^{-1})	η (100 s^{-1})
F-AA	11.68 ± 0.51	8.09 ± 0.23	8.06 ± 0.23
F-CA	7.04 ± 0.42	4.66 ± 0.21	3.86 ± 0.25
F-MA	13.45 ± 0.34 [d]	10.43 ± 0.36 [e]	8.47 ± 0.21 [f]
F-AB	11.97 ± 0.49	9.35 ± 0.41	8.45 ± 0.41
F-CB	7.49 ± 0.41	5.35 ± 0.23	4.35 ± 0.22
F-MB	17.86 ± 0.65 [a]	11.84 ± 0.20 [b]	9.55 ± 0.37 [c]

[a,b] $p \leq 0.01$ as compared to F-CB, F-AB; [c] $p \leq 0.05$ as compared to F-CB, F-AB; [d,e] $p \leq 0.01$ as compared to F-CA, F-AA; [f] $p \leq 0.05$ as compared to F-CA, F-AA. F-AA (SA; quercetin 0.4%), F-AB (SA; quercetin 0.7%), F-CA (CMC, quercetin 0.4%), F-CB (CMC, quercetin 0.7%), F-MA (MC, quercetin 0.4%), F-MB (MC, quercetin 0.7%).

It has been shown that viscosity is dependent on shear rate and shear stress and decreases as their values increase (Figure 3). Under the influence of the applied shear stress, the internal structure of the tested samples is destroyed, and the system starts to flow. Shear thinning was observed in all samples, particularly at low shear rates. The system shows pseudoplastic flow. Under the influence of increasing shear stress, the polymer particles arrange themselves in the direction of flow, which lowers the viscosity of the system. This strong shear thinning with a simultaneous decrease in viscosity throughout the experimental area confirms the good spreadability shown earlier in the test for the prepared formulations.

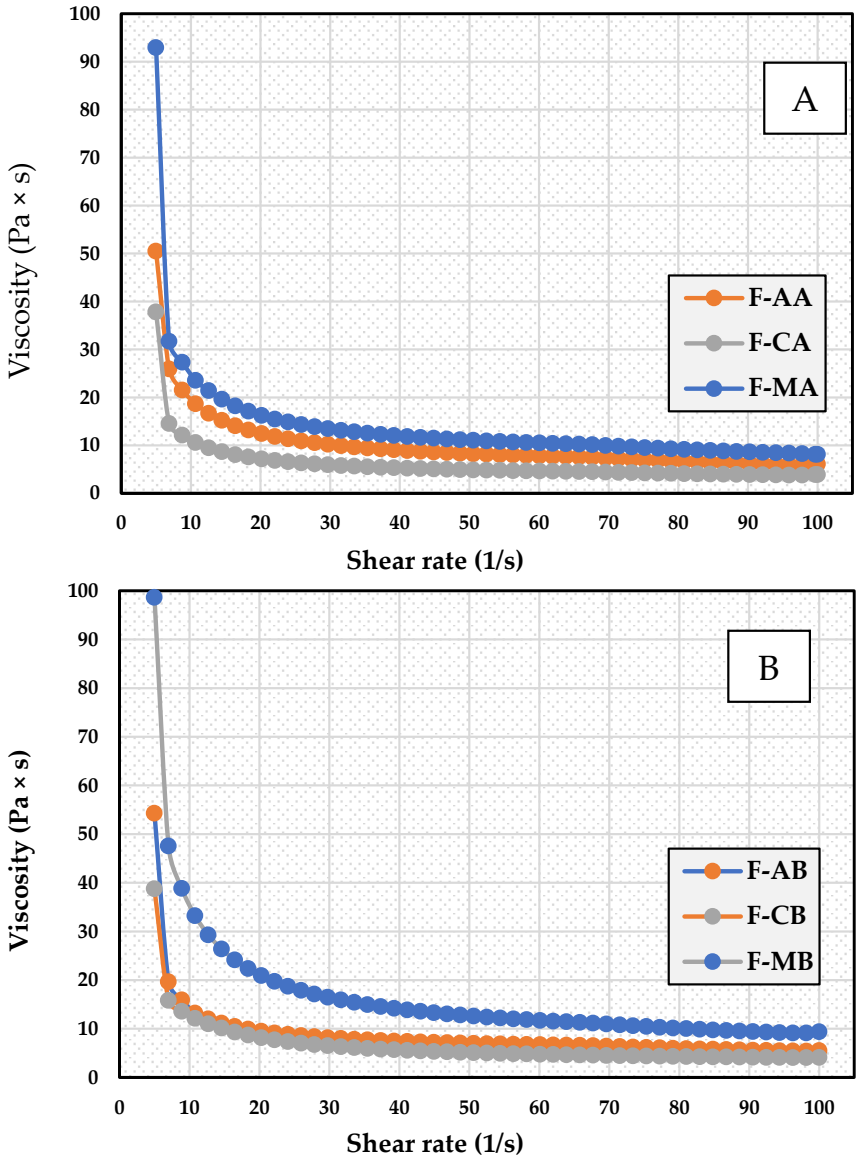

Figure 3. Viscosity curves for hydrogel: (**A**) F-AA, F-CA, F-MA; (**B**) F-AB, F-CB, F-MB. F-AA (SA; quercetin 0.4%), F-AB (SA; quercetin 0.7%), F-CA (CMC, quercetin 0.4%), F-CB (CMC, quercetin 0.7%), F-MA (MC, quercetin 0.4%), F-MB (MC, quercetin 0.7%).

Figure 4 shows rheograms illustrating flow under increasing and then decreasing shear stress. As can be seen in the figures, at the time of plotting the descending curve, the structure of the system is not yet completely reconstructed, so the curves do not coincide in the rheograms; hysteresis loops are then formed, indicating systems exhibiting thixotropy.

The calculated areas of the hysteresis loop for the prepared formulations were arranged in ascending order: 4588.51 (F-CB), 5799.10 (F-CA), 7814.95 (F-AA), 9314.87 (F-AB), 11650.96 (F-MB), 14114.72 (F-MA).

Yield strength is an important parameter used to characterize semi-solid formulations. It usually affects the spreadability and retention of formulations. A high value of yield stress indicates a reduction in spreadability and an increase in the ability to retain the formulation at the application site. In a study by Nair *et al.*, the yield stress for the formulation and control cream of N,N-diethyl-3-methylbenzamide (DEET) was 26.39 and 6.474 Pa, respectively, resulting in better spreadability of the cream than the hydrogel formulation [65]. A significant yield stress was required to break the microgel network present in the hydrogel, which contributed to the higher yield stress observed for the hydrogel compared to the cream. These findings were found to be consistent with the authors' results, where the MC

hydrogel had the lowest spreadability and highest yield stress (Figure 4). An increased retention capacity on the skin compared to SA and CMC hydrogels was observed in the permeation study of quercetin from F-MA and F-MB hydrogel.

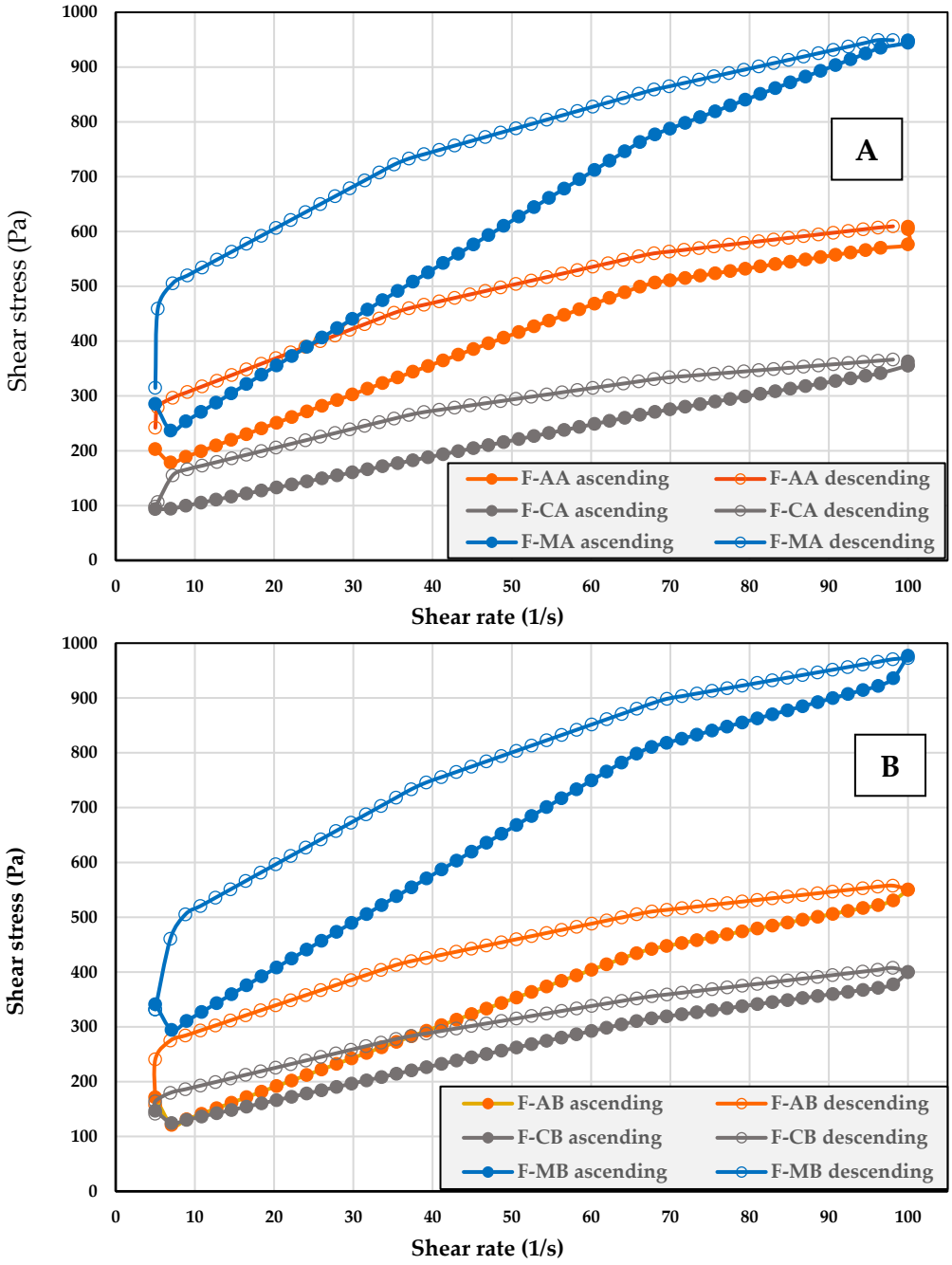

Figure 4. Flow curves hysteresis for hydrogel: (**A**) F-AA, F-CA, F-MA; (**B**) F-AB, F-CB, F-MB F-AA (SA; quercetin 0.4%), F-AB (SA; quercetin 0.7%), F-CA (CMC, quercetin 0.4%), F-CB (CMC, quercetin 0.7%), F-MA (MC, quercetin 0.4%), F-MB (MC, quercetin 0.7%).

3.5. Texture Analysis Parameters

Texture profile analysis is a means of assessing the mechanical properties of the polymers examined and their response to external pressure. The texture profile is described by textural parameters such as hardness, adhesiveness, cohesiveness, compressibility, and elasticity. Hardness is specified as the strength needed to cause a deformity. Specimens with greater hardness have poorer spreadability. Adhesiveness expresses the ability of the

test surface to bond with the probe surface. It allows the length of time the product will remain at the point of distribution—that is, on the skin—to be predicted [66].

Cohesion is evaluated as the relationship between the areas under the curve obtained in the first and second compression cycles. This value represents the inherent bond of load that must be defeated to distribute the product on the skin's surface. Compressibility is the work needed to distort the test specimen in the first squeezing cycle and represents the preservation of the formulation after the compressive load is taken away. Based on Yilmaz et al. [67], this value is associated with the elasticity of the specimen's [66]. The texture profiles and texture profile parameters obtained for the examined samples are shown in Figure 5 and Table 5.

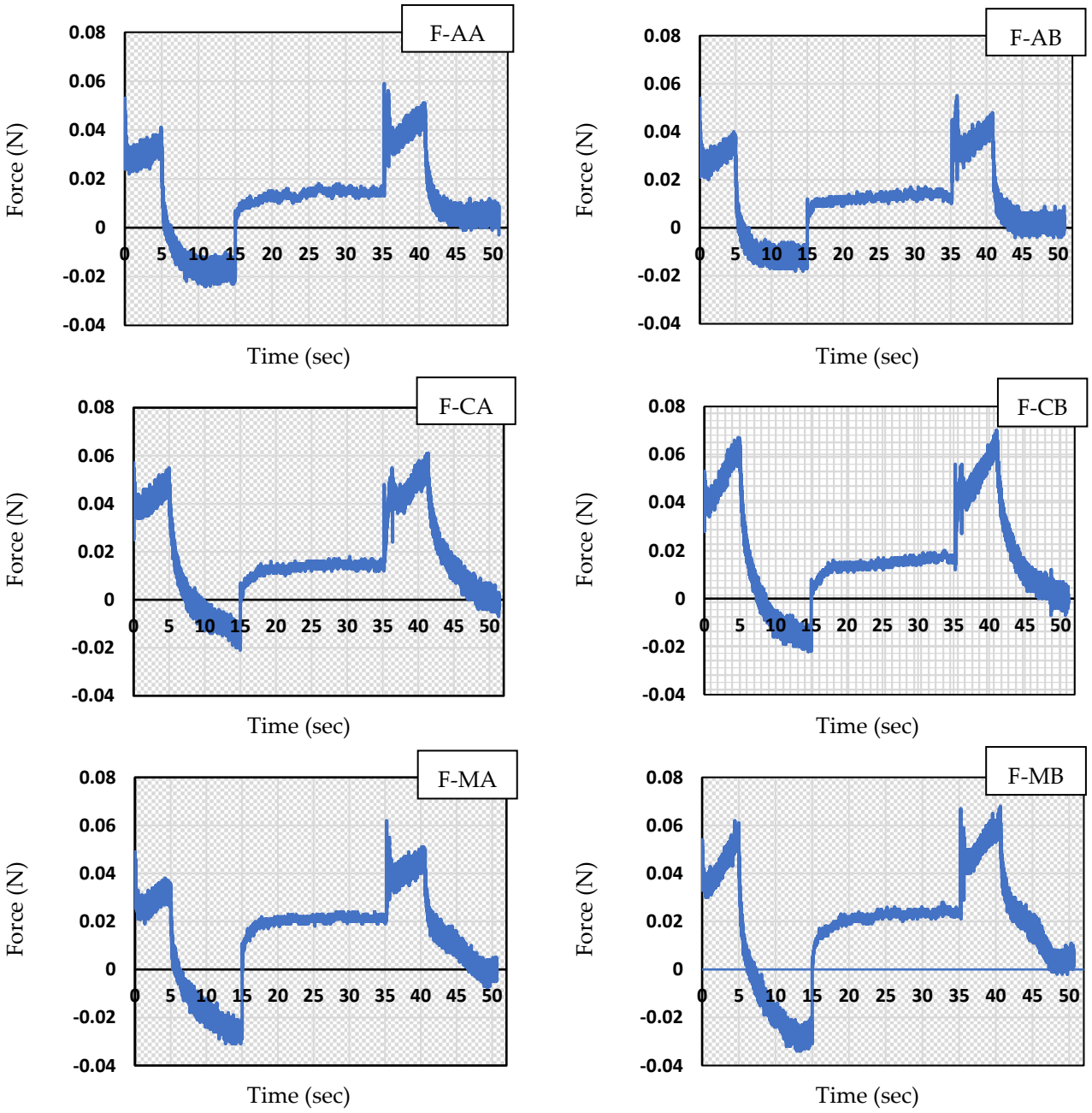

Figure 5. Texture profile analysis (TPA) in two compression/extension cycles of prepared hydrogel. F-AA (SA; quercetin 0.4%), F-AB (SA; quercetin 0.7%), F-CA (CMC, quercetin 0.4%), F-CB (CMC, quercetin 0.7%), F-MA (MC, quercetin 0.4%), F-MB (MC, quercetin 0.7%).

Table 5. Texture profile analysis comparing hardness, cohesiveness, adhesion, and elasticity for the obtained hydrogels containing different polymers (SA, MC, and CMC) and loaded with quercetin at two different concentrations; $n = 6$.

Formulation Code	Hardness (N)	Cohesiveness	Adhesiveness (mJ)	Elasticity
F-AA	0.0520 ± 0.001	2.316 ± 0.054 [a]	0.150 ± 0.050	0.649 ± 0.008 [a]
F-CA	0.0575 ± 0.001 [a]	1.314 ± 0.116 [a]	0.100 ± 0.000 [a]	0.868 ± 0.065 [a]
F-MA	0.0505 ± 0.002	2.698 ± 0.073	0.150 ± 0.050	0.583 ± 0.012
F-AB	0.0545 ± 0.001 [b]	2.127 ± 0.199	0.150 ± 0.050 [b]	0.665 ± 0.030 [b]
F-CB	0.0645 ± 0.003	1.306 ± 0.025 [b]	0.100 ± 0.000 [b]	0.816 ± 0.034 [b]
F-MB	0.0640 ± 0.003	2.157 ± 0.140	0.250 ± 0.050	0.580 ± 0.027

[a] $p \leq 0.05$ as compared to F-MA; [b] $p \leq 0.05$ as compared to F-MB. F-AA (SA; quercetin 0.4%), F-AB (SA; quercetin 0.7%), F-CA (CMC, quercetin 0.4%), F-CB (CMC, quercetin 0.7%), F-MA (MC, quercetin 0.4%), F-MB (MC, quercetin 0.7%).

In addition, it is evident that the type of polymer used in the developed formulation affected the resistance of the projected hydrogels.

The highest hardness among hydrogels containing a lower concentration of quercetin was determined for the CMC-based hydrogel to be 0.0575 ± 0.001, while the lowest for the MC-based hydrogel was 0.0505 ± 0.002. A slightly higher hardness than MC was observed for the SA-based hydrogel at 0.0520 ± 0.001. For hydrogels containing a higher concentration of quercetin, CMC-based and MC-based hydrogels showed similar hardnesses of 0.0645 ± 0.003 F-CB and 0.0640 ± 0.003 F-MB, respectively, while those based on SA were about 1.2 times lower (0.0545 ± 0.001). In all formulations, increasing the concentration of quercetin resulted in an increase in hardness, to the greatest extent for MC—about 1.3 times. The formulation containing CMC also showed the highest elasticity: 0.868 ± 0.065 (lower quercetin concentration) and 0.816 ± 0.034 (higher quercetin concentration). Meanwhile, the formulation containing MC showed the lowest elasticity. In this formulation, quercetin concentration did not affect the change in elasticity.

Inversely to the hardness at a lower quercetin concentration, the lowest cohesion value was observed for hydrogels with CMC (1.314 ± 0.116), as well as the lowest adhesion (0.100 ± 0.000). This confirmed the results obtained from the sensory evaluation of semi-solid formulations, in which CMC-based hydrogels had the lowest stickiness and adhesion. MC-containing hydrogels had the highest cohesiveness, although higher concentrations of quercetin slightly worsened their cohesiveness (by about 1.3-fold). Higher and similar adhesion was observed in ALG and MC-based formulations, while lower adhesion was shown for CMC. Increasing the concentration of quercetin significantly increased the adhesion of the MC-containing hydrogel (by about 1.7-fold), while the adhesion parameter was not affected in ALG- and CMC-based hydrogels.

Young's modulus is a criterion of a specimen's "rigidity" (mechanical responsiveness)—the capacity of a specimen to recover its initial conformation after distortion—and represents the amount of and distance between elastic segments [68]. As a result of the analysis, the values of Young's modulus (YM) and the stress and strain at failure of the sample were obtained. The tensile strength and Young's modulus are presented in Figure 6.

MC-based formulations showed the highest tensile strength: about 1.4-fold higher than the CMC-based hydrogel and about 1.5-fold higher than the SA-based formulation. In addition, a higher concentration of quercetin further increased the strength of the MC-containing hydrogel (by about 1.1-fold). In contrast, in CMC- and ALG-based formulations, the higher concentration slightly reduced the physical resistance of the formulation. The high tensile strength of the MC hydrogels showed consistency with the viscosity of these formulations, as the viscosity of MC-based hydrogels was the highest, and in turn, the higher concentration of quercetin gave this formulation the best adhesion. As a result, the F-MB formulation may be the most favorable in terms of adhesion to the skin, allowing the active ingredient to stay in contact with the skin for a longer period of time and act longer.

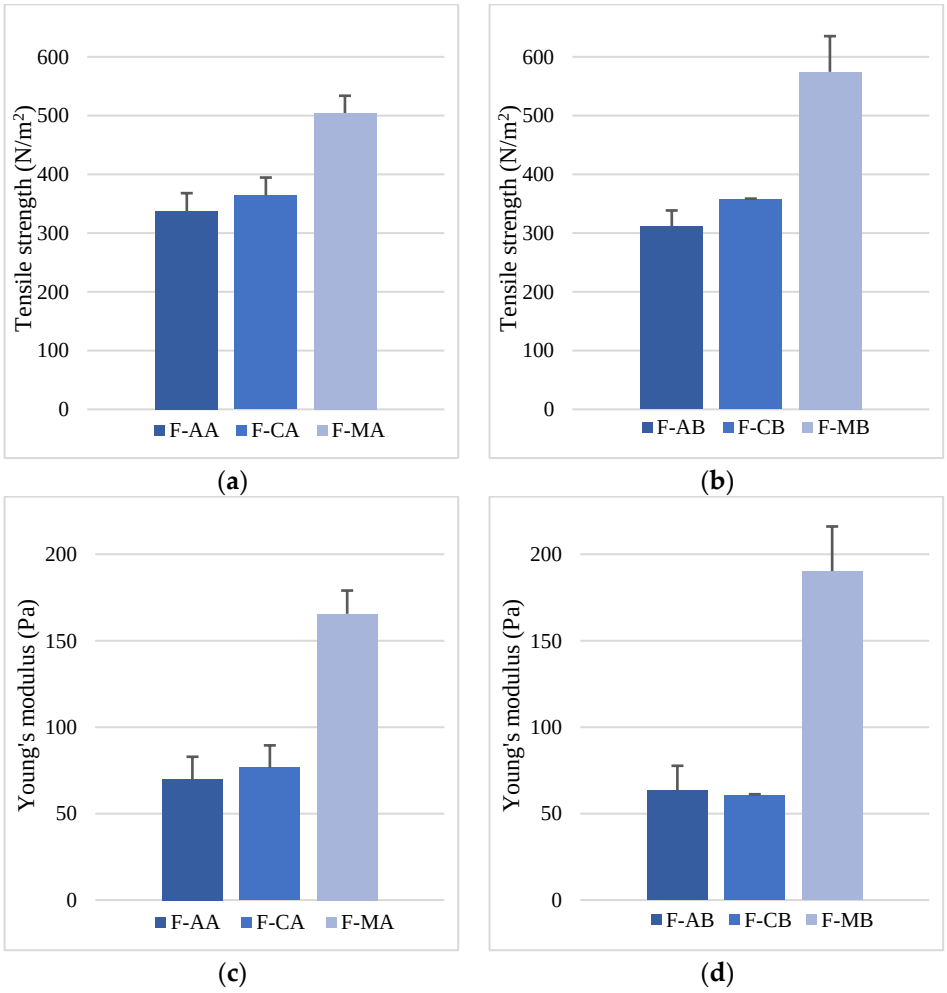

Figure 6. Comparison of: tensile strength profiles for hydrogels loaded with 0.4% quercetin (**a**) and hydrogels loaded with 0.7% quercetin (**b**); Young's modulus for hydrogels loaded with 0.4% quercetin (**c**); and hydrogels loaded with 0.7% quercetin (**d**). Up speed 1 mm/s, down speed 1 mm/s, distance 10 mm, the duration of experiment was 50 s. F-AA (SA; quercetin 0.4%), F-AB (SA; quercetin 0.7%), F-CA (CMC, quercetin 0.4%), F-CB (CMC, quercetin 0.7%), F-MA (MC, quercetin 0.4%), F-MB (MC, quercetin 0.7%).

In the formulations prepared, the greatest Young's modulus was noticed for MC as the hydrogel-forming polymer; the lowest Young's modulus was noticed for SA, and it was slightly higher for CMC. Increasing the concentration of quercetin increased the modulus of stiffness for MC, while the other hydrogels—with ALG and CMC—conversely decreased the Young's modulus. The MC-based hydrogel showed the highest tensile strength and the highest stiffness. Increasing the concentration of quercetin further favorably affected the strength parameters of the MC-based hydrogel.

3.6. Stability Studies

After one month of storage in the dark at 2 °C to 8 °C, the prepared gels were stable—no delamination or organoleptic changes were noted. The determined concentration of quercetin in the formulations was in accordance with the permissible limit and was above 90% of the initial content [69]. No physico-mechanical changes were found to affect their properties. Viscosity and texture parameters, determined after 28 days, were not significantly different from the values recorded on day 1. The stability data of stored quercetin preparations after 28 days are reported in Supplementary Materials (Tables S1–S3).

3.7. Ex Vivo Skin Permeation Studies

The results obtained in the in ex vivo permeation and retention study through porcine ear skin are shown in Table 6. The study showed that 24 h after hydrogel application to the skin, the amount of labelled quercetin in the acceptor fluid was low. The percentage of penetrated quercetin was 0.10%, 0.07%, and 0.16% of the total applied dose for F-AA, F-CA, and F-MA, respectively. After the application of formulations with higher concentrations of API in the hydrogel base, an increase of approximately 1.2 times for F-AB, 1.1 for (F-CB), and 1.2 (for F-MB) in the amount of skin permeation of the active ingredient was observed compared with F-AA, F-CA, and F-MA, respectively.

Table 6. Quercetin penetration (%) and retention (μg/cm^2) into porcine ear skin from hydrogels.

Formulation Code	Cumulative Amount of Flavonoid Permeated (%)	Flavonoid Retention (μg/cm^2) ± SD
F-AA	0.10 ± 0.02	4.21 ± 0.62 [c]
F-CA	0.07 ± 0.01	2.97 ± 0.26 [c]
F-MA	0.13 ± 0.02	7.88 ± 0.91 [a]
F-AB	0.12 ± 0.02	6.48 ± 0.73 [d]
F-CB	0.08 ± 0.01	4.63 ± 0.73 [d]
F-MB	0.16 ± 0.04	9.45 ± 0.89 [b]

[a] $p \leq 0.01$ as compared to F-AA, F-CA; [b] $p \leq 0.01$ as compared to F-AB, F-CB; [c] $p \leq 0.01$ as compared to F-MA, [d] $p \leq 0.01$ as compared to F-MB. F-AA (SA; quercetin 0.4%), F-AB (SA; quercetin 0.7%), F-CA (CMC, quercetin 0.4%), F-CB (CMC, quercetin 0.7%), F-MA (MC, quercetin 0.4%), F-MB (MC, quercetin 0.7%).

The results showed that quercetin from the F-MA and F-MB formulations was able to cross the stratum corneum at higher concentrations ($p \leq 0.01$) compared to the F-AA, F-AB, F-CA, and F-CB formulations. The retention of this flavonoid in the skin from MC-based formulations was significantly higher ($p \leq 0.01$) than formulations with lower quercetin content by 31.4% and 51% compared to F-AA and F-AB, respectively. A similar trend was observed for formulations with higher API content. Compared to F-AA and F-AB, the amount of drug retained in the skin reservoir was significantly higher ($p \leq 0.01$) for F-MB by 46.6% and 62.3%, respectively.

4. Discussion

The topic of substances of natural origin, mainly derived from plants, and their use in dermatological preparations applied to the skin, such as in the form of ointments, creams, and hydrogels, has recently been increasingly discussed. Particularly noteworthy are hydrogels, whose semi-solid consistency, spreadability, good mechanical properties, and other physical characteristics are due to their internal structure. This is a structure that is a combination of a solid (rigid) phase and a continuous (liquid) phase. Hydrogels are a three-dimensional network in which the solid phase is formed by suitable polymers and the liquid phase by water with dissolved substances. Their chemical structure allows for a gradual release of the API from the hydrogel matrix, which translates into a prolonged pharmacological effect. Advantageous features of this drug formulation include high biocompatibility, transparency, and easy wash-off [70]. Unfortunately, when applied to the skin, it dries quickly and can be irritating as a result. To prevent rapid drying, glycerol or propylene glycol is added to these bases.

The main barrier to the penetration of the active ingredient is the stratum corneum. In the case of topical administration, it is important to increase the passage of the API through the stratum corneum so that it is retained in the inner layers of the skin. The permeation of medicinal substances through the skin depends on many factors, such as the condition of the skin, the presence of absorption promoters, the physicochemical characteristics of the API, and the vehicle used in the dermatological preparation. Unfortunately, quercetin shows poor water solubility, higher metabolism, and poor bioavailability, which limits its therapeutic use. A number of works have addressed its topical delivery in the form of nanocarrier systems [71,72]. Transdermal delivery of quercetin from formulations can be

improved by the use of penetration enhancers such as dimethylformamide, L-menthol [73], diethylene glycol monoethyl ether [74], oxymatrine-fatty acid deep eutectic solvents [75], propylene glycol, and polyethylene glycol 400 [76].

In our study, DMSO was used as a transdermal quercetin transport enhancer. DMSO is a solvent with low toxicity and documented efficacy in the treatment of various skin injuries. It is also applied to enhancing the solubility of poorly soluble polar and non-polar molecules [77]. It is a potent penetrator of cell membranes and biological barriers, so it is used as a carrier to increase the permeability and absorption of actives substances.

The target site of quercetin action is the epidermis and dermis, where the disease process is taking place. After application, the drug should be released slowly, and systemic absorption should be zero or minimized. Our ex vivo permeation and retention results showed that quercetin from CMC-based formulations crossed the stratum corneum to a significantly higher degree ($p < 0.01$) compared to ALC- and MC-based formulations. Furthermore, the higher API content of the hydrogel substrate correlated with increased accumulation in the skin layers.

Kant et al. studied the influence of applying various doses of quercetin of 0.03, 0.1, and 0.3% on wound contraction in rats. Quercetin dissolved in DMSO (75%) was applied topically once a day for 20 days to wounds; the control group received DMSO alone. The application of the natural flavonoid at a dose of 0.3% was shown to be more beneficial in accelerating cutaneous wound healing. During the first week of treatment, increased levels of proliferating PCNA-positive cells, decreased TNF-α levels, and increased IL-10 expression were observed in the 0.3% quercetin-treated group compared to the 0.03%, 0.1% quercetin, and control groups, which, as a result, had a beneficial effect on the synthesis of collagen hydroxyproline and pro-alpha I chain [78].

A test by Dyja and Jankowski evaluated the influence of two solvents—propylene glycol and polyethylene glycol (PEG 400)—on the skin retention of quercetin. Propylene glycol was shown to be a more effective promoter of absorption than PEG 400. The amount of the flavonoid found in the skin was 1.47 times higher when propylene glycol was added to the semisolid base than PEG 400. No correlation was found between the kind of delivery systems used (gel, cream) and the dermal accumulation of quercetin [76].

In a study conducted on fresh Caucasian human skin, good penetration and retention of epigallocatechin-3-gallate and quercetin from green tea and G. biloba extracts contained in skin care preparations were found. The findings revealed that the flavonoids tested penetrated the skin while not reaching the receptor compartment. The highest amount of quercetin was determined in the viable epidermis (0.23 μg/cm^2) [79].

To study the penetration/retention of quercetin through porcine ear skin, Schwingel et al. incorporated this natural flavonoid into hydroxypropyl methylcellulose (HPMC) or chitosan (CS) hydrogels. The retention of quercetin in the skin layers of chitosan hydrogels has been shown to be more than twice that of HPMC. After 8 h, flavonoid retention in pig ear skin was 0.57 μg/cm^2 for HPMC and 1.42 μg/cm^2 for CS. It was noted that when 5% β-CD was added to the hydrogels, API penetration/retention rose to 1.95 μg/cm^2 for HPMC and 2.21 μg/cm^2 for CS. The authors did not detect this flavonoid in the receptor fluid [61].

Silva et al. investigated the antimicrobial efficacy of hydrogel membranes containing red propolis extract (RPE). The made hydrogels were based on 5% CMC and additionally with 0.5% and 1.0% citric acid. CMC was found to have a favorable effect on the release of phenolic compounds compared to the highly cross-linked 1% citric acid matrix. CMC with 0.5% citric acid as a membrane provided higher efficacy against *Staphylococcus aureus* and *Staphylococcus epidermidis* compared to the 1% citric acid cross-linked membrane. RPE-containing hydrogel membranes proved to be a stronger barrier to microorganisms that cause skin infections and can be used in the treatment of injured tissue [80].

5. Conclusions

The selection of raw materials forming the polymer matrix of a formulation is an important stage in the development of a dermatological formulation, determining their sensorial properties, rheological parameters, and texture profile. In the present study, we prepared hydrogels using different gelling agents (MC, CMC, and SA) containing quercetin and showed their good physico-mechanical properties and stability. MC-based formulations were selected as optimal in terms of mechanical properties—these formulations were characterized by higher textural parameters, except for elasticity. Ex vivo permeation and retention studies revealed that after 24 h, the highest amount of quercetin retained in the porcine skin reservoir was found for the MC-based formulation, followed by the SA-based and CMC-based formulations. For the MC-based formulations applied to the skin, containing a higher concentration of quercetin, its amount was 2.04 and 2.6 times higher compared to CMC-based and SA-based hydrogels, respectively. The formulation with MC as a gelling agent allows for longer contact of the active substance with the skin and thus better penetration. Thus, for formulations made with this carrier, a better therapeutic effect can be expected when applied to the affected skin.

Supplementary Materials: The following supporting information can be downloaded at: https://www.mdpi.com/article/10.3390/app13137826/s1. Table S1: Spreadability and pH of prepared quercetin hydrogels after one month of storage.; Table S2: Apparent viscosity prepared hydrogels depending on the shear rate (η) after one month of storage.; Table S3: Texture profile analysis comparing hardness, cohesiveness, adhesion and elasticity for the obtained hydrogels containing different polymers: SA, MC and CMC and loaded with quercetin at two different concentrations after one month of storage; n = 6.

Author Contributions: Conceptualization, B.S.-M. methodology, B.S.-M.; software, B.S.-M.; validation, B.S.-M.; formal analysis, B.S.-M.; investigation, B.S.-M. and W.S.; resources, B.S.-M. and B.D.; data curation, B.S.-M.; writing—original draft preparation, B.S.-M. and W.S.; writing—review and editing, B.S.-M.; visualization, B.S.-M. and W.S.; supervision, B.S.-M.; project administration, B.S.-M.; funding acquisition, B.S.-M. and B.D. All authors have read and agreed to the published version of the manuscript.

Funding: This research was funded by the Medical University of Silesia in Katowice, grant number PCN-1-100/N/1/F.

Institutional Review Board Statement: Not applicable.

Informed Consent Statement: Not applicable.

Data Availability Statement: Not applicable.

Conflicts of Interest: The authors declare no conflict of interest.

References

1. Anand David, A.V.; Arulmoli, R.; Parasuraman, S. Overviews of biological importance of quercetin: A bioactive flavonoid. *Pharmacogn. Rev.* **2016**, *10*, 84–89. [PubMed]
2. Seo, M.J.; Lee, Y.J.; Hwang, J.H.; Kim, K.J.; Lee, B.Y. The inhibitory effects of quercetin on obesity and obesity-induced inflammation by regulation of MAPK signaling. *J. Nutr. Biochem.* **2015**, *26*, 1308–1316. [CrossRef]
3. Li, D.; Jiang, C.; Mei, G.; Zhao, Y.; Chen, L.; Liu, J.; Tang, Y.; Gao, C.; Yao, P. Quercetin alleviates ferroptosis of pancreatic β cells in type 2 diabetes. *Nutrients* **2020**, *12*, 2954. [CrossRef] [PubMed]
4. Ghafouri-Fard, S.; Shabestari, F.A.; Vaezi, S.; Abak, A.; Shoorei, H.; Karimi, A.; Taheri, M.; Basiri, A. Emerging impact of quercetin in the treatment of prostate cancer. *Biomed. Pharmacother.* **2021**, *138*, 111548. [CrossRef]
5. Ebrahimpour, S.; Zakeri, M.; Esmaeili, A. Crosstalk between obesity, diabetes, and alzheimer's disease: Introducing quercetin as an effective triple herbal medicine. *Ageing Res. Rev.* **2020**, *62*, 101095. [CrossRef] [PubMed]
6. Guan, T.; Cao, C.; Hou, Y.; Li, Y.; Wei, X.; Li, S.; Jia, S.; Zhao, X. Effects of quercetin on the alterations of serum elements in chronic unpredictable mild stress-induced depressed rats. *Biometals* **2021**, *34*, 589–602. [CrossRef]
7. Wu, W.; Li, R.; Li, X.; He, J.; Jiang, S.; Liu, S.; Yang, J. Quercetin as an antiviral agent inhibits influenza A virus (IAV) entry. *Viruses* **2015**, *8*, 6. [CrossRef]

8. Khan, K.; Najmi, A.K.; Akhtar, M. A natural phenolic compound quercetin showed the usefulness by targeting inflammatory, oxidative stress markers and augment 5-ht levels in one of the animal models of depression in mice. *Drug Res.* **2019**, *69*, 392–400. [CrossRef]
9. Winnica, D.E.; Monzon, A.; Ye, S.; Vladar, E.K.; Saal, M.; Cooney, R.; Liu, C.; Sharma, S.; Holguin, F. Airway epithelial Paraoxonase-2 in obese asthma. *PLoS ONE* **2022**, *17*, e0261504. [CrossRef]
10. Cesarone, M.R.; Belcaro, G.; Hu, S.; Dugall, M.; Hosoi, M.; Ledda, A.; Feragalli, B.; Maione, C.; Cotellese, R. Supplementary prevention and management of asthma with quercetin phytosome: A pilot registry. *Minerva Med.* **2019**, *110*, 524–529. [CrossRef]
11. Lesjak, M.; Beara, I.; Simin, N.; Pintać, D.; Majkić, T.; Bekvalac, K.; Orčić, D.; Mimica-Dukić, N. Antioxidant and anti-inflammatory activities of quercetin and its derivatives. *J. Funct. Foods* **2018**, *40*, 68–75. [CrossRef]
12. Li, H.; Chen, F.J.; Yang, W.L.; Qiao, H.Z.; Zhang, S.J. Quercetin improves cognitive disorder in aging mice by inhibiting Nlrp3 inflammasome activation. *Food Funct.* **2021**, *12*, 717–725. [CrossRef] [PubMed]
13. Alkushi, A.G.R.; Elsawy, N.A.M. Quercetin attenuates, indomethacin-induced acute gastric ulcer in rats. *Folia Morphol.* **2017**, *76*, 252–261. [CrossRef] [PubMed]
14. Abdel-Tawab, M.S.; Mostafa Tork, O.; Mostafa-Hedeab, G.; Ewaiss Hassan, M.; Azmy Elberry, D. Protective effects of quercetin and melatonin on indomethacin induced gastric ulcers in rats. *Rep. Biochem. Mol. Biol.* **2020**, *9*, 278–290. [CrossRef]
15. Ma, Z.X.; Zhang, R.Y.; Rui, W.J.; Wang, Z.Q.; Feng, X. Quercetin alleviates chronic unpredictable mild stress-induced depressive-like behaviors by promoting adult hippocampal neurogenesis via FoxG1/CREB/ BDNF signaling pathway. *Behav. Brain Res.* **2021**, *406*, 113245. [CrossRef]
16. Grewal, A.K.; Singh, T.G.; Sharma, D.; Sharma, V.; Singh, M.; Rahman, M.H.; Najda, A.; Walasek-Janusz, M.; Kamel, M.; Albadrani, G.M.; et al. Mechanistic insights and perspectives involved in neuroprotective action of quercetin. *Biomed. Pharmacother.* **2021**, *140*, 111729. [CrossRef]
17. Jiang, Y.H.; Jiang, L.Y.; Wang, Y.C.; Ma, D.F.; Li, X. Quercetin attenuates atherosclerosis via modulating oxidized LDL-induced endothelial cellular senescence. *Front. Pharmacol.* **2020**, *11*, 512. [CrossRef]
18. Li, H.; Xiao, L.; He, H.; Zeng, H.; Liu, J.; Jiang, C.; Mei, G.; Yu, J.; Chen, H.; Yao, P.; et al. Quercetin attenuates atherosclerotic inflammation by inhibiting galectin-3-NLRP3 signaling pathway. *Mol. Nutr. Food Res.* **2021**, *65*, e2000746. [CrossRef]
19. Luo, X.; Weng, X.; Bao, X.; Bai, X.; Lv, Y.; Zhang, S.; Chen, Y.; Zhao, C.; Zeng, M.; Huang, J.; et al. A novel anti-atherosclerotic mechanism of quercetin: Competitive binding to KEAP1 via Arg483 to inhibit macrophage pyroptosis. *Redox Biol.* **2022**, *57*, 102511. [CrossRef]
20. Dehghani, F.; Sezavar Seyedi Jandaghi, S.H.; Janani, L.; Sarebanhassanabadi, M.; Emamat, H.; Vafa, M. Effects of quercetin supplementation on inflammatory factors and quality of life in post-myocardial infarction patients: A double blind, placebo-controlled, randomized clinical trial. *Phytother. Res.* **2021**, *35*, 2085–2098. [CrossRef]
21. Majewska, M.; Czeczot, H. Flavonoids in prevention and therapy of diseases. *Farm. Pol.* **2009**, *65*, 369–377.
22. Batiha, G.E.; Beshbishy, A.M.; Ikram, M.; Mulla, Z.S.; El-Hack, M.E.A.; Taha, A.E.; Algammal, A.M.; Elewa, Y.H.A. The pharmacological activity, biochemical properties, and pharmacokinetics of the major natural polyphenolic flavonoid: Quercetin. *Foods* **2020**, *9*, 374. [CrossRef]
23. Salehi, B.; Machin, L.; Monzote, L.; Sharifi-Rad, J.; Ezzat, S.M.; Salem, M.A.; Merghany, R.M.; El Mahdy, N.M.; Kılıç, C.S.; Sytar, O.; et al. Therapeutic potential of quercetin: New insights and perspectives for human health. *ACS Omega* **2020**, *5*, 11849–11872. [CrossRef] [PubMed]
24. Woźnicka, E.; Kuźniar, A.; Nowak, D.; Nykiel, E.; Kopacz, M.; Gruszecka, J.; Golec, K. Comparative study on the antibacterial activity of some flavonoids and their sulfonic derivatives. *Acta Pol. Pharm.* **2013**, *70*, 567–571. [PubMed]
25. Weng, Z.Y.; Zhang, B.D.; Asadi, S.; Sismanopoulos, N.; Butcher, A.; Fu, X.; Katsarou-Katsari, A.; Antoniou, C.; Theoharides, T.C. Quercetin is more effective than cromolyn in blocking human mast cell cytokine release and inhibits contact dermatitis and photosensitivity in humans. *PLoS ONE* **2012**, *7*, e33805. [CrossRef]
26. Park, E.J.; Kim, J.Y.; Jeong, M.S.; Park, K.Y.; Park, K.H.; Lee, M.W.; Joo, S.S.; Seo, S.J. Effect of topical application of quercetin-3-O-(2″-gallate)-alpha-l-rhamnopyranoside on atopic dermatitis in NC/Nga mice. *J. Dermatol. Sci.* **2015**, *77*, 166–172. [CrossRef]
27. Beken, B.; Serttas, R.; Yazicioglu, M.; Turkekul, K.; Erdogan, S. Quercetin improves inflammation, oxidative stress, and impaired wound healing in atopic dermatitis model of human keratinocytes. *Pediatr. Allergy Immunol. Pulmonol.* **2020**, *33*, 69–79. [CrossRef]
28. Bagde, A.; Patel, K.; Mondal, A.; Kutlehria, S.; Chowdhury, N.; Gebeyehu, A.; Patel, N.; Kumar, N.; Singh, M. Combination of UVB absorbing titanium dioxide and quercetin nanogel for skin cancer chemoprevention. *AAPS PharmSciTech* **2019**, *20*, 240. [CrossRef]
29. Nan, W.; Ding, L.; Shi, X.; Sui, X.-B. Topical use of quercetin-loaded chitosan nanoparticles against ultraviolet B radiation. *Front. Pharmacol.* **2018**, *9*, 826. [CrossRef]
30. Rajnochová Svobodová, A.; Ryšavá, A.; Čížková, K.; Roubalová, L.; Ulrichová, J.; Vrba, J.; Zálešák, B.; Vostálová, J. Effect of the flavonoids quercetin and taxifolin on UVA-induced damage to human primary skin keratinocytes and fibroblasts. *Photochem. Photobiol. Sci.* **2022**, *21*, 59–75. [CrossRef]
31. Zhu, X.; Li, N.; Wang, Y.; Ding, L.; Chen, H.; Yu, Y.; Shi, X. Protective effects of quercetin on UVB irradiation-induced cytotoxicity through ROS clearance in keratinocyte cells. *Oncol. Rep.* **2017**, *37*, 209–218. [CrossRef] [PubMed]
32. Chitkara, A.; Mangla, B.; Kumar, P.; Javed, S.; Ahsan, W.; Popli, H. Design-of-experiments (doe)-assisted fabrication of quercetin-loaded nanoemulgel and its evaluation against human skin cancer cell lines. *Pharmaceutics* **2022**, *14*, 2517. [CrossRef] [PubMed]

33. Mansi, K.; Kumar, R.; Narula, D.; Pandey, S.K.; Kumar, V.; Singh, K. Microwave-Induced CuO Nanorods: A comparative approach between curcumin, quercetin, and rutin to study their antioxidant, antimicrobial, and anticancer effects against normal skin cells and human breast cancer cell lines MCF-7 and T-47D. *ACS Appl. Bio Mater.* **2022**, *5*, 5762–5778. [CrossRef]
34. Caddeo, C.; Nacher, A.; Vassallo, A.; Armentano, M.F.; Pons, R.; Fernàndez-Busquets, X.; Carbone, C.; Valenti, D.; Fadda, A.M.; Manconi, M. Effect of quercetin and resveratrol co-incorporated in liposomes against inflammatory/oxidative response associated with skin cancer. *Int. J. Pharm.* **2016**, *513*, 153–163. [CrossRef] [PubMed]
35. Ali, H.; Dixit, S. Quercetin attenuates the development of 7, 12-dimethyl benz (a) anthracene (DMBA) and croton oil-induced skin cancer in mice. *J. Biomed. Res.* **2015**, *29*, 139–144. [PubMed]
36. Shin, E.J.; Lee, J.S.; Hong, S.; Lim, T.G.; Byun, S. Quercetin Directly Targets JAK2 and PKCδ and Prevents UV-Induced Photoaging in Human Skin. *Int. J. Mol. Sci.* **2019**, *20*, 5262. [CrossRef] [PubMed]
37. Aghamohammadi, M.; Zolghadr, L.; Nezhad, N.S.; Ahmadpour Yazdi, H.; Esfahani, A.J.; Gheibi, N. Investigating the effects of quercetin fatty acid esters on apoptosis, mechanical properties, and expression of ERK in melanoma cell line (A375). *Life Sci.* **2022**, *310*, 121007. [CrossRef]
38. Fu, J.; Huang, J.; Lin, M.; Xie, T.; You, T. Quercetin promotes diabetic wound healing via switching macrophages from M1 to M2 polarization. *J. Surg. Res.* **2019**, *246*, 213–223. [CrossRef]
39. Mi, Y.; Zhong, L.; Lu, S.; Hu, P.; Pan, Y.; Ma, X.; Yan, B.; Wei, Z.; Yang, G. Quercetin promotes cutaneous wound healing in mice through Wnt/β-catenin signaling pathway. *J. Ethnopharmacol.* **2022**, *290*, 115066. [CrossRef]
40. Wang, J.; Song, M.; Pan, J.; Shen, X.; Liu, W.; Zhang, X.; Li, H.; Deng, X. Quercetin impairs Streptococcus pneumoniae biofilm formation by inhibiting sortase A activity. *J. Cell. Mol. Med.* **2018**, *22*, 6228–6237. [CrossRef]
41. Sadeghi-Ghadi, Z.; Vaezi, A.; Ahangarkani, F.; Ilkit, M.; Ebrahimnejad, P.; Badali, H. Potent in vitro activity of curcumin and quercetin co-encapsulated in nanovesicles without hyaluronan against Aspergillus and Candida isolates. *J. Mycol. Med.* **2020**, *30*, 101014. [CrossRef] [PubMed]
42. Hanif, H.; Abdollahi, V.; Javani Jouni, F.; Nikoukar, M.; Rahimi Esboei, B.; Shams, E.; Vazini, H. Quercetin nano phytosome: As a novel anti-leishmania and anti-malarial natural product. *J. Parasit. Dis.* **2023**, *12*, 257–264. [CrossRef] [PubMed]
43. Bidone, J.; Argenta, D.F.; Kratz, J.; Pettenuzzo, L.F.; Horn, A.P.; Koester, L.S.; Bassani, V.L.; Simões, C.M.; Teixeira, H.F. Antiherpes activity and skin/mucosa distribution of flavonoids from achyrocline satureioides extract incorporated into topical nanoemulsions. *Biomed. Res. Int.* **2015**, *2015*, 238010. [CrossRef] [PubMed]
44. Li, X.; Yang, X.; Wang, Z.; Liu, Y.; Guo, J.; Zhu, Y.; Shao, J.; Li, J.; Wang, L.; Wang, K. Antibacterial. antioxidant and biocompatible nanosized quercetin-PVA xerogel films for wound dressing. *Colloids Surf. B Biointerfaces* **2022**, *209*, 12175. [CrossRef]
45. Cikrikci, S.; Mert, B.; Oztop, M.H. Development of ph sensitive alginate/gum tragacanth based hydrogels for oral insulin delivery. *J. Agric. Food Chem.* **2018**, *66*, 11784–11796. [CrossRef] [PubMed]
46. Rioux, Y.; Fradette, J.; Maciel, Y.; Bégin-Drolet, A.; Ruel, J. Biofabrication of sodium alginate hydrogel scaffolds for heart valve tissue engineering. *Int. J. Mol. Sci.* **2022**, *23*, 8567. [CrossRef]
47. Liu, C.; Qin, W.; Wang, Y.; Ma, J.; Liu, J.; Wu, S.; Zhao, H. 3D printed gelatin/sodium alginate hydrogel scaffolds doped with nano-attapulgite for bone tissue repair. *Int. J. Nanomed.* **2021**, *16*, 8417–8432. [CrossRef]
48. Yao, Z.; Qian, Y.; Jin, Y.; Wang, S.; Li, J.; Yuan, W.E.; Fan, C. Biomimetic multilayer polycaprolactone/sodium alginate hydrogel scaffolds loaded with melatonin facilitate tendon regeneration. *Carbohydr. Polym.* **2022**, *277*, 118865. [CrossRef]
49. Anghel, N.; Dinu, M.V.; Zaltariov, M.; Pamfil, D.; Spiridon, I. New cellulose-collagen-alginate materials incorporated with quercetin, anthocyanins and lipoic acid. *Int. J. Biol. Macromol.* **2021**, *181*, 30–40. [CrossRef]
50. Shafei, S.; Khanmohammadi, M.; Heidari, R.; Ghanbari, H.; Taghdiri Nooshabadi, V.; Farzamfar, S.; Akbariqomi, M.; Sanikhani, N.S.; Absalan, M.; Tavoosidana, G. Exosome loaded alginate hydrogel promotes tissue regeneration in full-thickness skin wounds: An in vivo study. *J. Biomed. Mater. Res. A* **2020**, *108*, 545–556. [CrossRef]
51. Wang, T.; Yi, W.; Zhang, Y.; Wu, H.; Fan, H.; Zhao, J.; Wang, S. Sodium alginate hydrogel containing platelet-rich plasma for wound healing. *Colloids Surf. B Biointerfaces* **2023**, *222*, 113096. [CrossRef] [PubMed]
52. Naeem, A.; Yu, C.; Zhu, W.; Chen, X.; Wu, X.; Chen, L.; Zang, Z.; Guan, Y. Gallic acid-loaded sodium alginate-based (polyvinyl alcohol-co-acrylic acid) hydrogel membranes for cutaneous wound healing: Synthesis and characterization. *Molecules* **2022**, *27*, 8397. [CrossRef] [PubMed]
53. Garg, D.; Matai, I.; Agrawal, S.; Sachdev, A. Hybrid gum tragacanth/sodium alginate hydrogel reinforced with silver nanotriangles for bacterial biofilm inhibition. *Biofouling* **2022**, *38*, 965–983. [CrossRef]
54. Mali, K.K.; Dhawale, S.C.; Dias, R.J.; Dhane, N.S.; Ghorpade, V.S. Citric acid crosslinked carboxymethyl cellulose-based composite hydrogel films for drug delivery. *Indian J. Pharm. Sci.* **2018**, *80*, 657–667. [CrossRef]
55. Niemczyk-Soczynska, B.; Gradys, A.; Kolbuk, D.; Krzton-Maziopa, A.; Rogujski, P.; Stanaszek, L.; Lukomska, B.; Sajkiewicz, P. A methylcellulose/agarose hydrogel as an innovative scaffold for tissue engineering. *RSC Adv.* **2022**, *2*, 26882–26894. [CrossRef] [PubMed]
56. Bonetti, L.; De Nardo, L.; Farè, S. Thermo-responsive methylcellulose hydrogels: From design to applications as smart biomaterials. *Tissue Eng. Part B Rev.* **2021**, *27*, 486–513. [CrossRef]
57. Lim, S.J.; Lee, J.H.; Piao, M.G.; Lee, M.K.; Oh, D.H.; Hwangdu, H.; Quan, Q.Z.; Yong, C.S.; Choi, H.G. Effect of sodium carboxymethylcellulose and fucidic acid on the gel characterization of polyvinylalcohol-based wound dressing. *Arch. Pharm. Res.* **2010**, *33*, 1073–1081. [CrossRef] [PubMed]

58. Kanikireddy, V.; Varaprasad, K.; Jayaramudu, T.; Karthikeyan, C.; Sadiku, R. Carboxymethyl cellulose-based materials for infection control and wound healing: A review. *Int. J. Biol. Macromol.* **2020**, *164*, 963–975. [CrossRef]
59. Lee, I.S.; Yang, H.M.; Kim, J.W.; Maeng, Y.J.; Lee, C.W.; Kang, Y.S.; Rang, M.J.; Kim, H.Y. Terminology development and panel training for sensory evaluation of skin care products including aqua cream. *J. Sens. Stud.* **2005**, *20*, 421–433. [CrossRef]
60. Siemiradzka, W.; Franczyk, A.; Bułaś, L.; Dolińska, B. Somatotropin penetration testing from formulations applied topically to the skin. *Appl. Sci.* **2023**, *13*, 2588. [CrossRef]
61. Schwingel, L.C.; Bianchi, S.E.; Zorzi, G.K.; Gonçalves, P.; Teixeira, H.F.; Bassani, V.L. Quercetin and 3-O-methylquercetin in vitro skin layers permeation/retention from hydrogels: Why only a methoxy group difference determines different behaviors? *J. Pharm. Pharmacol.* **2019**, *71*, 733–745. [CrossRef] [PubMed]
62. Schürer, N. pH and Acne. *Curr. Probl. Dermatol.* **2018**, *54*, 115–122. [CrossRef] [PubMed]
63. Rippke, F.; Berardesca, E.; Weber, T.M. pH and Microbial Infections. *Curr. Probl. Dermatol.* **2018**, *54*, 87–94.
64. Lynde, C.; Tan, J.; Skotnicki, S.; Beecker, J.; Claveau, J.; Li, M.K.; Rao, J.; Salsberg, J.; Sauder, M.B.; Zip, C. Skin Surface pH. *J. Drugs Dermatol.* **2019**, *18*, 214.
65. Sreedharan Nair, R.; Rahman, H.; Kong, M.X.; Tan, X.Y.; Chen, K.Y.; Shanmugham, S. Development and rheological evaluation of DEET (N,N-diethyL-3-methylbenzamide) microparticles loaded hydrogel for topical application. *Turk. J. Pharm. Sci.* **2021**, *18*, 352–359. [CrossRef]
66. Osmałek, T.; Milanowski, B.; Froelich, A.; Górska, S.; Białas, W.; Szybowicz, M.; Kapela, M. Novel organogels for topical delivery of naproxen: Design, physicochemical characteristics and in vitro drug permeation. *Pharm. Dev. Technol.* **2017**, *22*, 521–536. [CrossRef] [PubMed]
67. Yilmaz, M.T.; Karaman, S.; Dogan, M.; Yetim, H.; Kayacier, A. Characterization of O/W model system meat emulsions using shear creep and creep recovery tests based on mechanical simulation models and their correlation with texture profile analysis (TPA) parameters. *J. Food Eng.* **2012**, *108*, 327–336. [CrossRef]
68. Franzén, H.M.; Draget, K.I.; Langebäck, J.; Nilsen-Nygaard, J. Characterization and properties of hydrogels made from neutral soluble chitosans. *Polymers* **2015**, *7*, 373–389. [CrossRef]
69. U.S. Pharmacopeial Convention. *United States Pharmacopeia, 32*; U.S. Pharmacopeial Convention: Rockville, MD, USA, 2009; Volume 2, pp. 2282–2284.
70. Yang, Y.; Xu, L.; Wang, J.; Meng, Q.; Zhong, S.; Gao, Y.; Cui, X. Recent advances in polysaccharide-based self-healing hydrogels for biomedical applications. *Carbohydr. Polym.* **2022**, *283*, 119161. [CrossRef]
71. de Barros, D.P.C.; Santos, R.; Reed, P.; Fonseca, L.P.; Oliva, A. Design of quercetin-loaded natural oil-based nanostructured lipid carriers for the treatment of bacterial skin infections. *Molecules* **2022**, *27*, 8818. [CrossRef]
72. Sapino, S.; Ugazio, E.; Gastaldi, L.; Miletto, I.; Berlier, G.; Zonari, D.; Oliaro-Bosso, S. Mesoporous silica as topical nanocarriers for quercetin: Characterization and in vitro studies. *Eur. J. Pharm. Biopharm.* **2015**, *89*, 116–125. [CrossRef] [PubMed]
73. Huang, C.; Wang, H.; Tang, L.; Meng, F. Penetration enhancement of menthol on quercetin through skin: Insights from atomistic simulation. *J. Mol. Model.* **2019**, *25*, 235. [CrossRef] [PubMed]
74. Scalia, S.; Franceschinis, E.; Bertelli, D.; Iannuccelli, V. Comparative evaluation of the effect of permeation enhancers, lipid nanoparticles and colloidal silica on in vivo human skin penetration of quercetin. *Skin Pharmacol. Physiol.* **2013**, *26*, 57–67. [CrossRef] [PubMed]
75. Li, B.; Xiao, T.; Guo, S.; Wu, Y.; Lai, R.; Liu, Z.; Luo, W.; Xu, Y. Oxymatrine-fatty acid deep eutectic solvents as novel penetration enhancers for transdermal drug delivery: Formation mechanism and enhancing effect. *Int. J. Pharm.* **2023**, *637*, 122880. [CrossRef] [PubMed]
76. Dyja, R.; Jankowski, A. The effect of additives on release and in vitro skin retention of flavonoids from emulsion and gel semisolid formulations. *Int. J. Cosmet. Sci.* **2017**, *39*, 442–449. [CrossRef] [PubMed]
77. Karim, M.; Boikess, R.S.; Schwartz, R.A.; Cohen, P.J. Dimethyl sulfoxide (DMSO): A solvent that may solve selected cutaneous clinical challenges. *Arch. Dermatol. Res.* **2022**, *21*, 588–600. [CrossRef]
78. Kant, V.; Jangir, B.L.; Kumar, V.; Nigam, A.; Sharma, V. Quercetin accelerated cutaneous wound healing in rats by modulation of different cytokines and growth factors. *Growth Factors* **2020**, *38*, 105–119. [CrossRef]
79. dal Belo, S.E.; Gaspar, L.R.; Maia Campos, P.M.; Marty, J.P. Skin penetration of epigallocatechin-3-gallate and quercetin from green tea and Ginkgo biloba extracts vehiculated in cosmetic formulations. *Skin Pharmacol. Physiol.* **2009**, *22*, 299–304. [CrossRef]
80. Silva, V.C.; Silva, A.M.; Basílio, J.A.; Xavier, J.A.; do Nascimento, T.G.; Naal, R.M.; del Lama, M.P.; Leonelo, L.A.; Mergulhão, N.L.; Maranhão, F.C.; et al. New insights for red propolis of alagoas—Chemical constituents, topical membrane formulations and their physicochemical and biological properties. *Molecules* **2020**, *25*, 5811. [CrossRef]

Disclaimer/Publisher's Note: The statements, opinions and data contained in all publications are solely those of the individual author(s) and contributor(s) and not of MDPI and/or the editor(s). MDPI and/or the editor(s) disclaim responsibility for any injury to people or property resulting from any ideas, methods, instructions or products referred to in the content.